

# The influence of speed and cooling system setting on the thermal deformation of spindle

WeiLi Zhong · WenHsin Hsieh

Received: date / Accepted: date

**Abstract** In precision machining, the thermal error has always been recognized as the most significant error, generally accounting for 40-70% of all errors. In a typical machine tool, the components that generate thermal error usually include the spindle, spindle slide, column, bottom bed and feed system, while the heat is generated by the rotation of the spindle motor and the feed system. Here, we analyze the correlation between temperature rise and thermal deformation by regression analysis. According to the previous paper and industrial experience, we selected thirteen temperature points that are most relevant to the thermal deformation of the spindle system for measurement. In addition, the cooling liquid inlet and outlet from the outside will affect the spindle system, as well as the bracket temperature specially selected for more precise calculation of the deformation. Also, we conduct three steps (Fuzzy clustering, Pearson and Spearman correlation, Multiple regression) to know the relation between temperature rise and thermal deformation. The results show that we can predict the thermal deformation of the machine tool tip within an error of  $7\mu\text{m}$ , which meet the industrial criterion. It means that we can provide the machine tool controller with timely compensation to reduce the machining error.

**Keywords** Machine tool spindle · Thermal error · Temperature-sensitive point · Fuzzy clustering · Correlation · Regression

WeiLi Zhong · WenHsin Hsieh  
College of Engineering, Peking University  
Tel.: +86-010-82524866  
Fax: +86-010-82524866  
E-mail: qq994478@pku.edu.cn

## 1 Introduction

During the operation process of machine tools, uneven heating of the components and complex temperature field cause thermal deformation, which leads to the relative position change between the tool and the workpieces. Thermal error has become the most important source of machine errors, especially for precision machining, thermal error accounts for about 40-70%[1]. Thermal error compensation technology is an effective and economical method to reduce machining error and improve the accuracy of machine tools[2]. The scheme of a typical machine tool is shown in Fig.1. Many research papers presented various methods of compensation of described thermal behaviour of machine tools. Brecher et al.[3] describes common strategies. Statistical approach using small number of temperature sensors can be easily applied on the machine,[4,5]. All these strategies use overall machine deformation. In general, this measurement cannot bring information about detailed behaviour of machine parts.

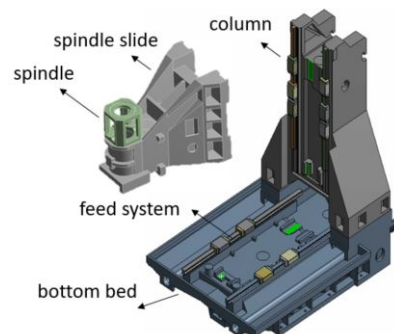


**Fig. 1** The scheme of a typical machine tool

In Fig.2, as the processing time increased, the thermal deformation was dominated by the spindle and the framework respectively. In the first 50 minutes, the thermal deformation rose rapidly. The thermal deformation was caused by the temperature rise of the spindle. In 50 and 150 minutes, the heat of the spindle and the motor was gradually transferred to the spindle slide, the column and other framework parts, so that these framework parts began to produce negative thermal deformation. The thermal deformation of these framework parts and the thermal deformation of the spindle offset each other. After 150 Minutes, the thermal deformation of the spindle had reached a steady state. Other framework parts (such as spindle slide, column, bottom bed, etc.) were far away from the heat source and had a large thermal inertia, so they had not reached the thermal equilibrium, and the temperature continued to rise, resulting in the increase of the thermal deformation (negative value), so that the thermal deformation of the tool tip continued to decline, even to negative thermal deformation. In order to correctly estimate the thermal deformation of the tool tip, the analyst of the spindle and framework parts must be clearly controlled.

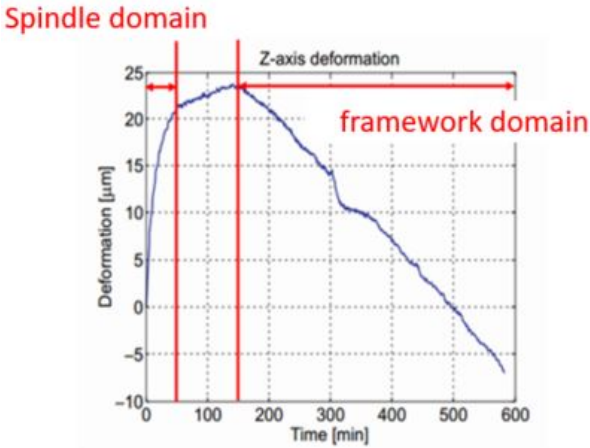


Fig. 2 Machine tool its tool tip Z-axis deformation

In the past, researchers analyzed the thermal compensation of the whole machine. The correlation between thermal deformation and temperature rise was not correct because the superposition of several thermal deformation factors. Therefore, to solve the complex problem of the structure and heat transfer of the machine tool, we focus on the spindle. Also, we conduct three steps (Fuzzy clustering, Pearson and Spearman correlation, Multiple regression) to build the spindle thermal compensation equation.

## 2 Experimental Set-up and Design

### 2.1 Experimental Set-up

Our experimental equipment was built to be the same as the industry as much as possible. Fig.3 and Fig.4 show four types of the spindle according to the driving mode, Belt type, Gear type, Built-in type, straight type.

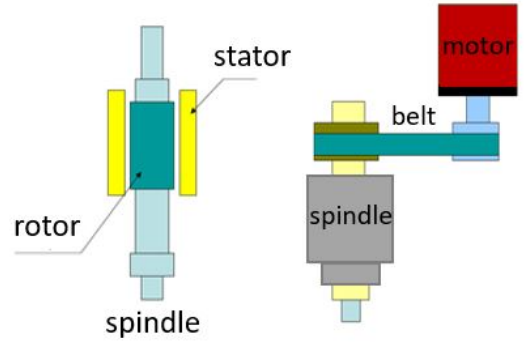


Fig. 3 Built-in type and Belt type

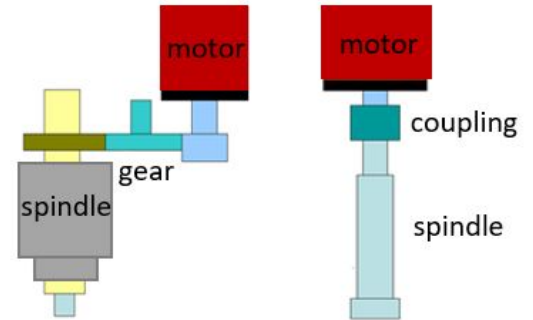


Fig. 4 Gear type and Straight type

The spindle is a component for holding the cutter and cutting. It needs to be operated for a long time. Different spindle types we pick may affect the results. Here, we briefly describe advantages and weaknesses. The advantage of gear type spindle is that it can transmit high torque and has good heavy cutting ability. Its disadvantage is that the speed is limited by the design of gear and it is not easy to improve. The advantage of the belt type spindle is that the vibration is smaller and it is easy to assemble. Its disadvantage is that the noise and the belt tension is not easy to control. The advantage of built-in type spindle is that it has low vibration and good dynamic rotation accuracy. Its disadvantage is that the temperature rise is too high. The straight type spindle its motor is located above the

spindle. The motor and the spindle are connected by a high rigidity gapless coupling. The rotation of the motor is transmitted to the spindle through the coupling and its speed is higher than the Gear type. Compared with the belt type, the noise is much smaller. Also, it is good for controlling temperature rise. Nowadays, most of machine tools adopt the straight type spindle except some special machining. We used the straight type spindle for our experimental results.

The independent spindle system used in this study was the high-speed spindle model used in Secto: straight type 101A. As shown in Table 1, the specification was driven by asynchronous servo motor, with the speed of up to 12000rpm and the maximum power of 11kw. The two diagonal contact bearings were configured in the form of back-to-back (O-shape arrangement) and fixed-fixed way. The spindle was supported on the base by the bracket, driven by the motor, cooled by the oil cooling system.

**Table 1** Specifications of the independent spindle equipment

equipment	brand	model number
spindle	Setco	101a
coupling	SKF	SKF7014CE
cooling system	Harbor	HBO-250PTSBM4-409
dryer system	SMC	IDF8E-20
controller system	LNC	†
tool	†	BT40

The temperature measurement used in this study were data acquisition card NI9213 and E-type thermocouples. The thermal displacement of each axis and the height change of the base of the spindle were using the capacitance displacement sensor and data acquisition card NI9239, and to measure the temperature rise of the rotary tool by using the thermal imager. The model number and specification of measuring equipment were shown in Table 2. The accuracy of NI9213 is  $0.25^{\circ}C$ , E-type  $\pm 1^{\circ}C$ , thermal imager  $\pm 2^{\circ}C$ , capacitance displacement sensor  $96\mu m$ , NI9239 was  $0.014V$ .

**Table 2** Measuring Equipment

variable	brand	model	accuracy
temperature	NI OMEGA	DAQ9213 E-type	$0.25^{\circ}C$ $\pm 1^{\circ}C$
tool	CHCT	P384-20	$\pm 2^{\circ}C$
displacement	NI LION.P	DAQ9239 CPL230	$0.014V$ $96\mu m$

## 2.2 Experimental Design

In this study, according to ISO230-3, a set of spindle temperature rise thermal deformation experimental equipment will be established to understand the spindle heat transfer phenomenon. Fig.5 shows the real independent spindle equipment. It can be divided into three parts: temperature measurement system, thermal deformation measurement system and experimental condition, which will be discussed in the following subsections.

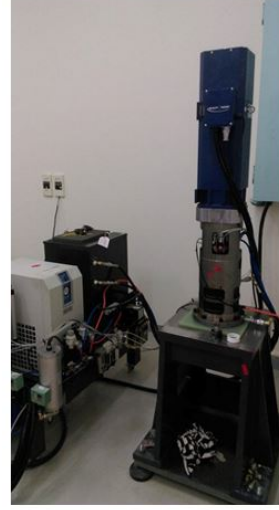


**Fig. 5** Independent spindle equipment

### 2.2.1 Temperature measurement system

In terms of measuring equipment, we used the thermal couple (TC) and two data acquisition cards NI9213 to measure the temperature. In order to see the overall situation of the spindle, thirty two temperature points were measured in total. However, as shown in Fig.6 and Fig.7, thirteen points which was most related to the thermal deformation had been selected for introduction. The other nineteen points were not temperature sensitive points because of the low correlation with the thermal compensation equation. The TC1-TC4 were the inside of the front bearing and TC5-TC7 were the measuring points of the rear bearing. TC8 and TC9 were the inlet and outlet temperature of the measured coolant, TC10-TC13 were the side of the measuring platform, the cylinder of the platform and the cylinder of the external displacement sensor, and TC13 was the room temperature.

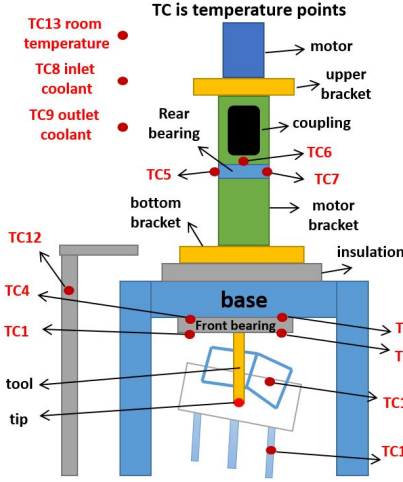


Fig. 6 Independent spindle system diagram



Fig. 7 Real independent spindle system

### 2.2.2 Thermal deformation measurement system

In the measurement of the thermal deformation, we used capacitance displacement sensor. There were four terms to be defined for the spindle thermal deformation measurement system: (A) Deformation of the internal platform (B) deformation of outside cylinder (C) deformation measured by DS2 (D) deformation measured by DS1.

First, deformation of the internal platform referred to the deformation of the platform with DS1 placed in the experiment due to the temperature rise. Second, deformation of outside cylinder referred to the deformation of the cylinder with DS2 installed in the experiment due to the temperature rise. The deformation measured by DS2 was the measurement of the distance change relative to the Z-axis. If the value was positive, it meant that the spindle went up. We needed to compensate the real machine tool tip deformation, so we put a minus sign in front of it. Deformation of the spin-

dle system (C)(D) and the deformation of the platform (A) and cylinder (B) had an equation describing machine tool tip as follows:

$$TCP = -(C) + (D) - (A) - (B)$$

where TCP was the thermal deformation on the Z-axis.

The spindle was fixed on the bottom bracket and the downward expansion of its bottom bracket was defined as a negative value. We knew that the deformation of the machine tool tip of the spindle should be calculated by (DS1) subtracting the base upward expansion amount (DS2). Furthermore, the expansion of outside cylinder and internal platform also needed to be adjusted. We demonstrate a series of calculation as follow:

$$(A) = \alpha_1 \cdot \Delta T_{10} \cdot L_1 + \alpha_2 \cdot \Delta T_{11} \cdot L_1$$

$$(B) = \alpha_3 \cdot \Delta T_{12} \cdot L_3$$

where  $\alpha$  meant coefficient of thermal expansion,  $\Delta T$  was temperature rise of TC10-TC12, and (C) and (D) were the value measured by capacitance displacement sensor, as shown in Fig.8.

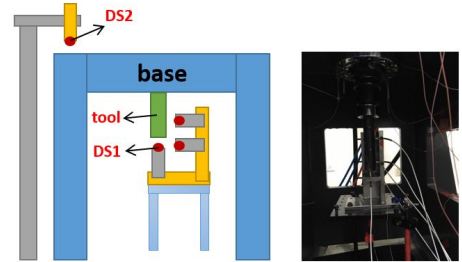


Fig. 8 Real independent spindle system

### 2.2.3 Experimental condition

In order to thoroughly understand the characteristics of the spindle, there were two experiments in total[6]. The first one was fixed speed experiment, three speeds were equipped with two kinds of ambient temperature (open air conditioner or not). In order to find the repeatability of each condition, we had done two times, total of twelve sets of data, the second was variable speed, open air conditioner, total of two sets of data, as shown in Table 3.

Under the fixed speed experiment of the spindle, the maximum speed of the spindle was 30%, 60% and 90%. The speed value was 3600, 7200 and 10800 rpm, respectively, for two hours of rotation. The purpose of this experiment is to fully understand the performance of the spindle at constant rotating speed through a

range from low to high. In addition, the ambient temperature was whether we opened air conditioner or not. The purpose is to explore whether room temperature is controlled or not the deformation of machine tool tip error in the factory. Furthermore, the thermal deformation fitting equations of the training group are also established.

The second was variable speed of the spindle measurement. The spindle speed changed every 20 minutes, from 30%, 60%, 90% and no operation in sequence. The first, whether there was the same temperature rise trend with constant speed. The second, testing thermal deformation fitting equations, i.e. checking the equation constructed under the constant speed whether was correct or not. When the temperature rises under variable speed as input, we want to compare how much the error between the actual and we predicted. If the error meet the industrial requirement, it represents our method is acceptable. Note that here no operation does not mean shutting down the machine, the cooling system still operates but motor stops rotating. It is more closed to standby.

**Table 3** Experimental condition

constant speed			
speed	3600rpm	7200rpm	10800rpm
condition	Air × 2	Air × 2	Air × 2
	No × 2	No × 2	No × 2
totaltimes	12		
variable speed			
speed	3600rpm-7200rpm-10800rpm-standby		
condition	Air × 2		
totaltimes	22		

### 3 Experimental results

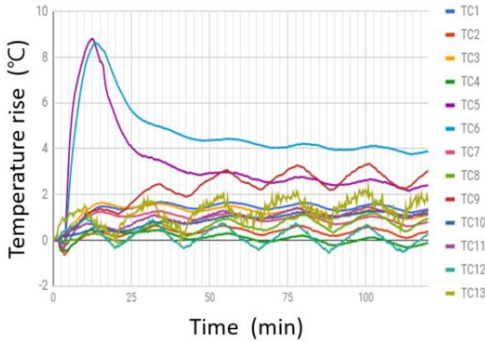


**Fig. 9** Constant speed 10800rpm No air, T0 at 27.47°C

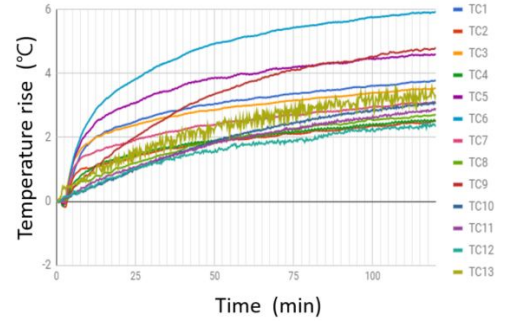


**Fig. 10** Constant speed 10800rpm air, T0 at 22.03°C

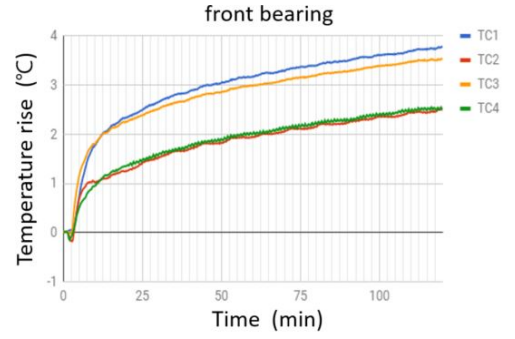


**Fig. 11** Constant speed 10800rpm No air, T0 at 27.47°C

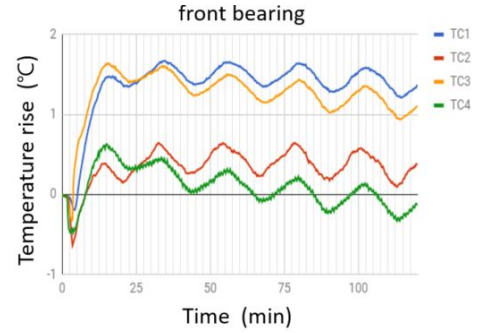


**Fig. 12** Constant speed 10800rpm air, T0 at 22.03°C

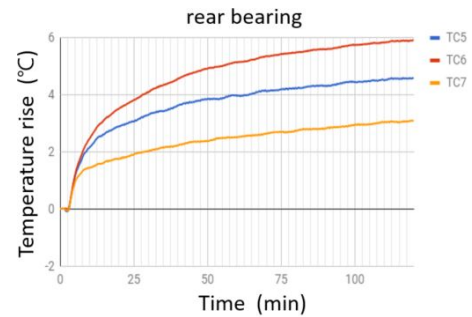


**Fig. 13** Constant speed 10800rpm No air, T0 at 27.47°C



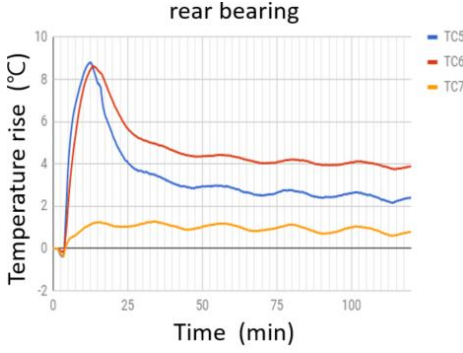


Fig. 14 Constant speed 10800rpm air, T0 at 22.03°C

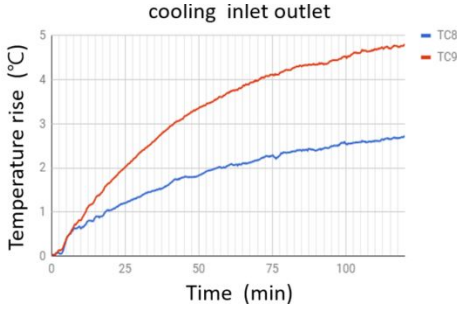


Fig. 15 Constant speed 10800rpm No air, T0 at 27.47°C

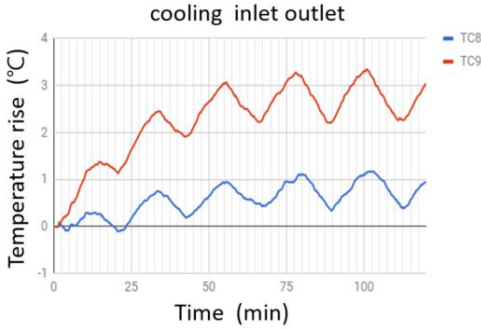


Fig. 16 Constant speed 10800rpm air, T0 at 22.03°C

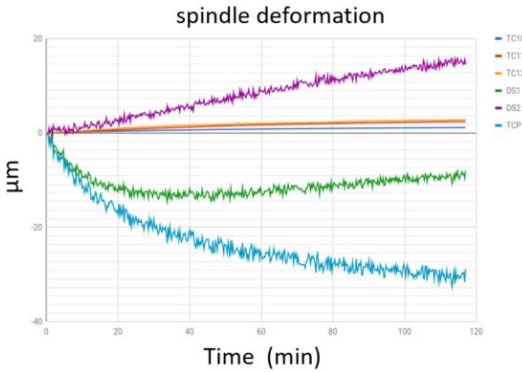


Fig. 17 Constant speed 10800rpm No air, T0 at 27.47°C

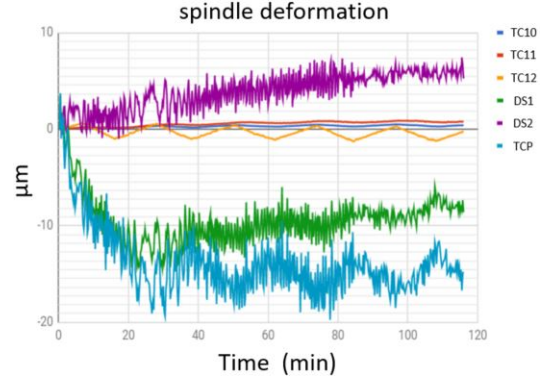


Fig. 18 Constant speed 10800rpm air, T0 at 22.03°C

The experimental results here only show that 10800 rpm constant speed no air-conditioner, 10800rpm constant speed air-conditioner and variable speed condition. The temperature rises more dramatically under 10800rpm constant speed no air-conditioner. The characteristics of machine tool are more relatively prominent and good for observation. We explain more details what the experimental result meaning. In Section 3.1 gives constant speed 10800rpm No air, T0 at 27.47°C. Section 3.2 demonstrates constant speed 10800rpm air, T0 at 22.03°C. Section 3.3 compares constant speed 10800rpm No air and air. Section 3.4 shows the variable speed condition result.

### 3.1 Constant speed 10800rpm No air, T0 at 27.47°C

As shown in Fig.9, the temperature rise of the measuring point under the non constant temperature environment. The temperature rise of the measuring point is more significant, and then it reaches thermal equilibrium with the ambient temperature. We can see the internal platform and outside cylinder TC10-TC12 was affected by increasing ambient temperature. Furthermore, ambient temperature TC13 rises due to the heat discharged by the spindle motor rotation. Fig.11 shows that the front bearing is under no air conditioner. The temperature of the measuring point decreases in the early stage due to oil gas omen, then rises rapidly, and the temperature of the front bearing gradually reaches the balance with the ambient temperature in twelve minutes, and the temperature rise slope slows down. Fig.13 shows that the rear bearing temperature rise and it is the most significant measurement point. The maximum temperature rise is close to 6°C, and the temperature rise trend is the same as front bearing. In Fig.15, the cooling system is set to change with the ambient temperature, the ambient temperature gradually rise due to the non-constant temperature state under

no air condition, so the coolant also change. Outlet coolant temperature rise is bigger than inlet because the coolant is used to bring out the heat of machine. Finally, in Fig.17, the machine tool tip deformation which we calculated went down about  $30\mu\text{m}$ .

### 3.2 Constant speed 10800rpm air, T0 at $22.03^{\circ}\text{C}$

As shown in Fig.10, the temperature rise of the measuring point under the constant temperature environment. The temperature rise of the measuring point is not significant, and it performs fluctuation to the ambient temperature. Also, we can see the internal platform and outside cylinder TC10-TC12 fluctuate by ambient temperature. Furthermore, ambient temperature TC13 is based on the the air conditioner, so the ambient temperature is controlled in a temperature range, and the temperature just rise slightly even if the heat released by the spindle. In Fig.12, the temperature of the measuring point decreases in the early stage due to oil gas omen, then rises rapidly, and it gradually reaches the balance in 12 minutes, and the temperature rise slope fluctuates. In Fig.14, the rear bearing temperature rise trend is the same as front bearing, but TC6 and TC7 have problems in the measurement, because the rear bearing has a water jacket to cover the point we measured and it is affected by the waste heat, so the temperature rises rapidly at the beginning. In Fig.16, the cooling system is set to change with the ambient temperature, and air conditioner temperature is in a range, so the coolant fluctuates instead of just rising. Finally, in Fig.18, the machine tool tip deformation was minus  $15\mu\text{m}$  which is lower than that of no air conditioner.

### 3.3 Compare constant speed 10800rpm No air and air

As shown in Fig.9 and Fig.10, the most obvious difference between the two is the final equilibrium temperature, no air condition temperature reached  $6^{\circ}\text{C}$ , air condition was  $2-4^{\circ}\text{C}$ . No air condition temperature rise reached steadily while the air condition reached with fluctuation. In Fig.11 and Fig.12, the difference is whether the equilibrium temperature fluctuate or not. In Fig.13 and Fig.14, although we can explain as previous, the rear bearing is the closest to spindle motor, so under air condition, the temperature rise was be controlled i.e. the temperature rise dropped quickly after 25 minutes. In Fig.14 and Fig.15, the fluctuation is obvious, and it can be attributed to two reasons. One is the measurement method and the other is air conditioner. We plunge the thermal couple into the coolant

directly and temperature is in a range under air conditioner. In Fig.17 and Fig.18, the most important thing is how much the machine tool tip deformation goes down. The reason why the deformation is much smaller than no air conditioner is that the air conditioner cool the machine at any time, reducing the thermal expansion, and reducing the deformation of the machine tool tip. Therefore, we hope to process machining under constant temperature, because it is the most efficiently to reduce thermal error.

### 3.4 Variable speed condition result

In Fig.19, the temperature rise of the measuring point under the air conditioner. The temperature rise of the total measuring point mainly follows with the change of the rotating speed, and has a fluctuation phenomenon. The internal platform and outside cylinder TC10-TC12 temperature rise is affected by the ambient temperature, but the influence of the variable speed is not great at this place, which is similar to the result of the constant speed of the air conditioner, and has the same fluctuation phenomenon in the temperature rise. Furthermore, ambient temperature TC13 is controlled by the air conditioner in a temperature range to vibrate. However, due to the influence of the rotating speed of the spindle and air conditioner, the room temperature will show periodic oscillation. In Fig.20, the temperature of the measuring point decreases at the early stage due to the oil gas omen, and then increases with the change of the speed respectively, and reaches the thermal equilibrium with the coolant at different temperatures. In Fig.21, the temperature rise of the rear bearing is the same as the front bearing. The temperature rises first, then slows down, and reaches the thermal equilibrium with the coolant, but the temperature rise slopes is bigger than front bearing because closer to the motor. In Fig.22, since the cooling system is set to change with ambient temperature, the ambient temperature is controlled in a range under the air conditioner. Therefore, the temperature of the cooling system changes with it, and it will appear period due to spindle speed and vibration due to air conditioner. In Fig.23, the emergency button is not used, so that the coolant is still cooling in standby state, so that the temperature returns to the original temperature, and the machine tool tip deformation will return to the original position. The whole process is presented periodically. In addition, there will be tool loading and unloading phenomenon from 10800rpm to the standby state and from standby state to 3600rpm, so the machine tool tip deformation of the Z-axis is very large. If we look more details, we can find the machine tool tip

deformation is familiar with respective constant speed experimental results.

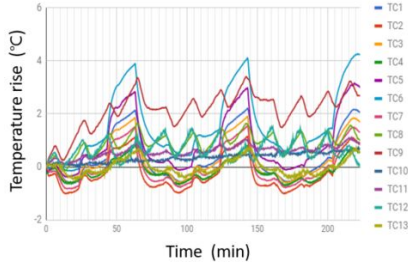


**Fig. 19** 3600-7200-10800rpm-standby, T0 at 21.59°C

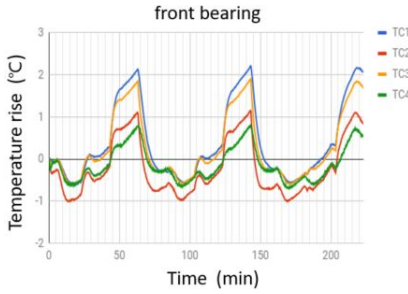


**Fig. 20** 3600-7200-10800rpm-standby, T0 at 21.59°C

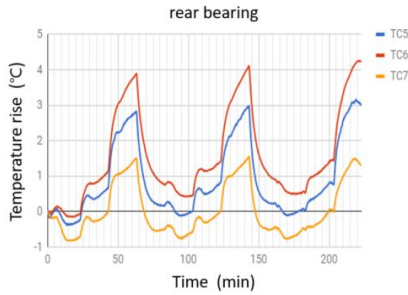


**Fig. 21** 3600-7200-10800rpm-standby, T0 at 21.59°C

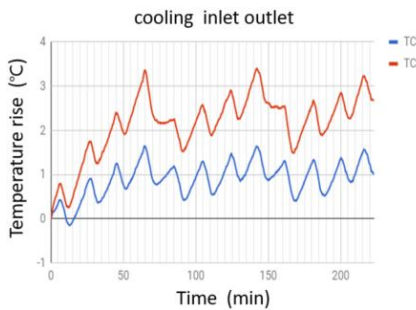


**Fig. 22** 3600-7200-10800rpm-standby, T0 at 21.59°C

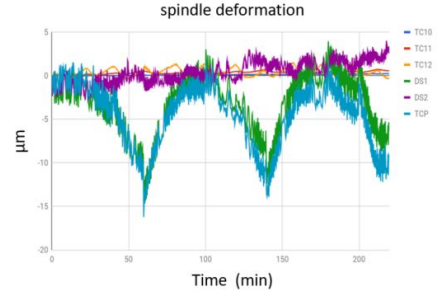


**Fig. 23** 3600-7200-10800rpm-standby, T0 at 21.59°C

#### 4 Data analysis and discussion

The most important thing here is to find out the relation between the deformation of the machine tool tip and the temperature rise, and then build the thermal compensation equation[7]. Furthermore, testing the thermal compensation equation by variable speed to know the error between prediction deformation and real deformation. In Fig.24, we do not consider the thermal deformation on the X-axis and Y-axis because the even heat expansion. We only consider the deformation of Z-axis[8]. In Fig.2, after twenty five minutes, we need to consider the thermal deformation on the X-axis and Y-axis because the heat expansion of the framework.

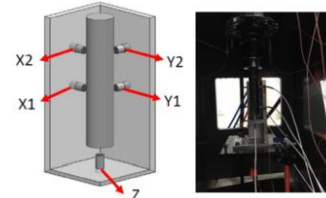


**Fig. 24** X-Y-Z axis sensor

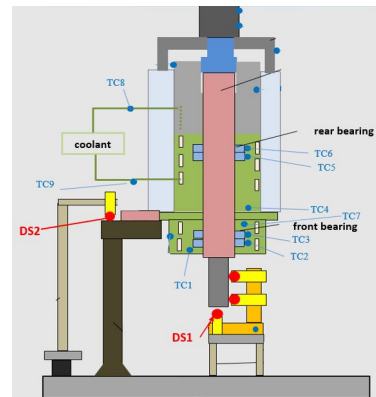


**Fig. 25** Temperature points in fuzzy clustering



#### 4.1 Fuzzy clustering

In Fig.25 and Fig.26, we process the data analysis step by step. First, we carry out the Fuzzy C-means clustering. The reason for this is that after the group division, we pick out one point to represent each group's temperature rise state. Physically, it is simplified to only one temperature point, and the temperature rise is only based on that point. Mathematically, the advantage is that it can reduce the parameters we need to consider in the thermal compensation equation. FCM algorithm is shown as follows:

$$\min_C \sum_{i=1}^n \sum_{j=1}^c w_{ij}^m \|x_i - c_j\| \quad (1)$$

$$w_{ij} = \frac{1}{\sum_{k=1}^c \left( \frac{\|x_i - c_j\|}{\|x_i - c_k\|} \right)^{\frac{2}{m-1}}} \quad (2)$$

where  $X \in \{x_1, \dots, x_n\}$  represents the nine temperature points in Fig.26. The algorithm returns a list of  $c$  cluster centres  $C \in \{c_1, \dots, c_c\}$  which was divided into three groups. The first group include TC1-TC4 and TC7. The second group is TC5 and TC6. The third group is TC9. TC8 is not included in the group because it is dominated by the cooling system and has low correlation with the spindle. It can be found that the clustering result is highly correlated with the actual location of the point.

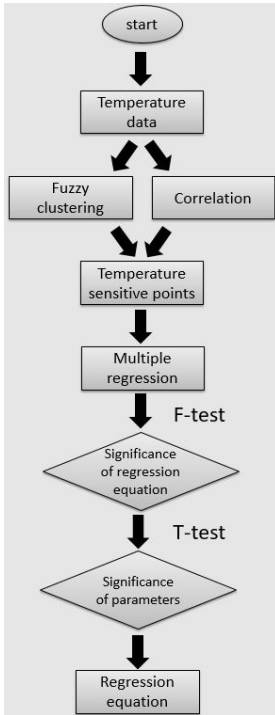


**Fig. 26** The steps of data analysis

#### 4.2 Temperature sensitive points and Correlation

In the second step, we make Pearson correlation between the machine tool tip deformation and eight temperature points. We can see which temperature points are more relative to spindle deformation. Fig.27 shows the result of correlation coefficient. We combine the first step and the second step, and pick out the temperature sensitive points. After we pick out the highest correlation coefficient among the same group, the result is TC1 in the first group, TC6 in second group, and TC9 in third group. Pearson correlation is shown as follows:

$$r_{xy} = \frac{n \sum x_i y_i - \sum x_i \sum y_i}{\sqrt{n \sum x_i^2 - (\sum x_i)^2} \sqrt{n \sum y_i^2 - (\sum y_i)^2}} \quad (3)$$

where  $r_{xy}$  is Pearson correlation coefficient between  $x$  and  $y$ ,  $n$  is number of observations,  $x_i$  is the value of temperature rise,  $y_i$  is value of machine tool tip deformation.

	TC1	TC2	TC3	TC4	TC5	TC6	TC7	TC8	TC9
$r_{xy}$	-0.96	-0.95	-0.93	-0.87	-0.7	-0.85	-0.93	-0.59	-0.71

**Fig. 27** The result of correlation coefficient

#### 4.3 Build the thermal compensation equation

In the third step, we conduct multiple regression analysis. After we pick out the three temperature sensitive points, the sensitive points are the variable in thermal compensation equation. We use F-test to find out which thermal compensation equation we perform the best, mostly in two order to four order. The t-statistic leave out the bad variable in the best thermal compensation equation. We need to conduct cross validation to see the residual error because sometimes it was not the best thermal compensation equation, after doing t-statistic might become the best fit equation. The independent variable parameters of multiple linear regression model based on the least squares estimation are shown as follows:

$$\hat{y}_i = b_0 + b_1 x_{i1} + b_2 x_{i2} + \dots + b_m x_{im} + \varepsilon_i (i = 1, 2, \dots, n)$$

$$F = \frac{ESS/m}{RSS/(n-m-1)}$$

$$TSS = RSS + ESS(\hat{y}_i - \bar{y})^2$$

$$ESS = \sum_{i=1}^n (y_i - \hat{y}_i)^2 \quad RSS = \sum_{i=1}^n (y_i - \bar{y})^2$$

where TSS is the overall square of regression equation, ESS is the regression square, RSS is the residual square,  $b_i (i = 1, 2, \dots, n)$  is the actual measurement values of dependent variable,  $\bar{y}$  is the mean of  $y_i (i = 1, 2, \dots, n)$ ,  $\hat{y}_i (i = 1, 2, \dots, n)$  is the estimate values of the regression equation,  $m$  is the degree of freedom (DOF) of ESS,  $(n-m-1)$  is the DOF of RSS. Then, t statistic:

$$t_i = \frac{b_i}{\sigma \sqrt{q_{i+1}}}, (i = 1, 2, \dots, m)$$

$$\sigma = \sqrt{\frac{RSS}{(n-m-1)}}$$

where  $b_i$  is parameters of equation,  $\sigma$  is residuals,  $q_{i+1}$  is the  $(i+1)$  th diagonal element of regression equation coefficient matrix A. Finally, in Fig.28-31, we can get each training result and the training thermal compensation equation.

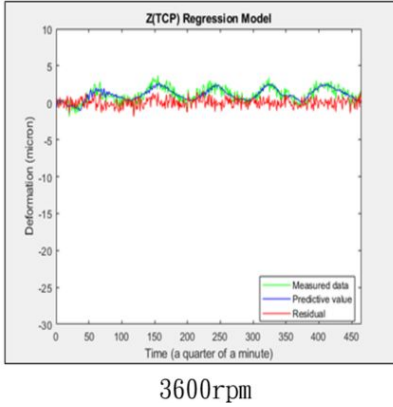


Fig. 28 3600rpm fit circumference air conditioner

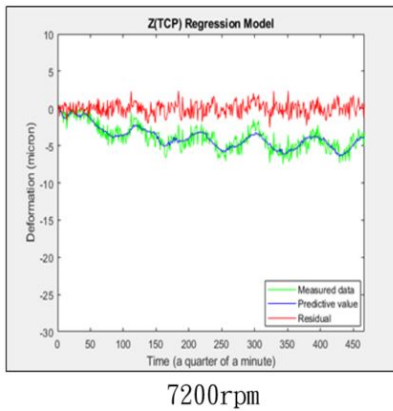


Fig. 29 7200rpm fit circumference air conditioner

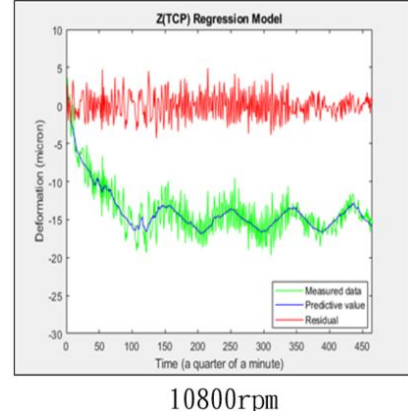


Fig. 30 10800rpm fit circumference air conditioner

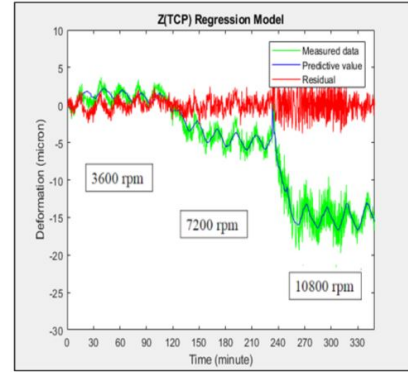


Fig. 31 total fit circumference air conditioner

$$E = b_0 + b_1 T1 + b_2 T6 + b_3 T8 + b_4 T1^2 + b_5 T6^2 + b_6 T9^2 + b_7 T1 T6 + b_8 T1 T9 + b_{10} T1^3 + b_{11} T6^3 + b_{12} T9^3 + b_{13} T1^2 T6 + b_{14} T1^2 T9 + b_{15} T6^2 T1 + b_{16} T6^2 T9 + b_{17} T9^2 T1 + b_{18} T9^2 T6 + b_{19} T1 T6 T9 \quad (4)$$

The training thermal compensation equation is above equation (4), Where E is the machine tool tip deformation,  $b_0$  to  $b_{19}$  is coefficient, T1, T6, T9 is temperature rise data.

#### 4.4 Testing compensation equation and discussion

In Fig.20-22, we obtain not only the variable speed spindle characteristic, but also an overall testing data. We can believe testing data is that the real industry process machining. In Fig 31, we get the training thermal compensation equation. We use the variable speed temperature rise as input to equation (4) and get output as prediction for machine tool tip deformation. Finally, we compare the real machine tool tip deformation (Fig.23) with the predictions of machine tool tip

deformation by our method. The compared result is shown in Fig.32, it is acceptable because the error is under  $7\mu\text{m}$ , which is adopted in industry.

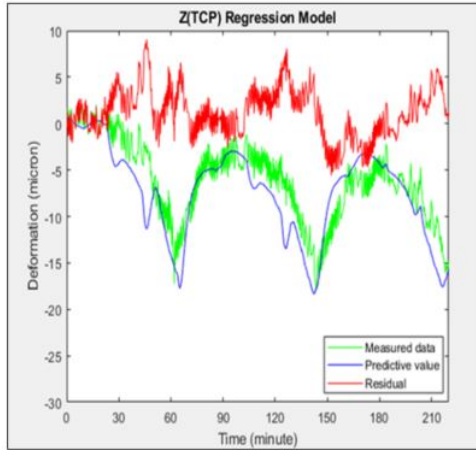


**Fig. 32** Compared result air conditioner

The training data or the testing data is under air conditioner in our experiments. The performance under no air conditioner is also adopted in industry. We completely observe the temperature rise of independent spindle in different conditions, and provide a set of methods to analyze the relation between temperature rise and thermal deformation. Furthermore, it is helpful to industry that providing the machine tool controller with timely compensation to reduce the machining error. There are two things to be noted. First, under no air conditioner machining is in mostly traditional industry, otherwise having air conditioner controlled is also existing, like machining chip enterprise. It is said that one more zero machining error after the decimal point, one more zero the value we get before the decimal point. Second, we do not consider the whole machine circumstance, as shown in Fig.2, the thermal deformation of the whole machine is complicate. We can figure out this problem by decomposition of the whole machine, and our study group team are going on that direction. Fortunately, we have solved the problem before 25 minutes process machining. And it is really helpful to the later study, because we have totally known the spindle characteristic which is one of main heat source.

## 5 Conclusion

By decomposition of the whole machine, we focus on one heat source, i.e. the spindle. We provide a set of method to deal with our problem by taking Fuzzy clus-

tering, Pearson and Spearman correlation, Multiple regression to find out the relation between temperature rise and thermal deformation, i.e. the thermal compensation equation. The accuracy of thermal deformation of the machine tool tip between we predict and the real is lower than  $7\mu\text{m}$ , which is acceptable in the industry. It means that we can provide the machine tool controller with timely compensation to reduce the machining error and prove that our study is worthwhile.

**Acknowledgements** Thanks for the experimental equipment provided by Tongtai enterprise.

## References

1. Guo Hua Zhou, Application design of tool machine, Book, 2014
2. En-ming, Miao, et al. Temperature-sensitive point selection of thermal error model of CNC machining center. The International Journal of Advanced Manufacturing Technology 74.5-8 (2014): 681-691.
3. Ramesh R, Mannan MA, Poo AN. Error compensation in machine tools - a review Part II: thermal errors. International Journal of Machine Tools and Manufacture 2000;40:1257-84
4. Lee JH, Yang SH. Statistical optimization and assessment of a thermal error model for CNC machine tools. International Journal of Machine Tools and Manufacture 2002;42:147-55.
5. Du ZC, Yang JG, Yao ZQ. Modeling approach of regression orthogonal experiment design for the thermal error compensation of a CNC turning center. Journal of Materials Processing Technology 2002;129:619-23.
6. VYROUBAL, Jiri. Compensation of machine tool thermal deformation in spindle axis direction based on decomposition method. Precision Engineering, 2012, 36.1: 121-127.
7. SARHAN, Ahmed AD. Investigate the spindle errors motions from thermal change for high-precision CNC machining capability. The International Journal of Advanced Manufacturing Technology, 2014, 70.5-8: 957-963.
8. VYROUBAL, J. Using the spindle cooling temperature as a tool for compensating the thermal deformation of machines. Acta Polytechnica, 2010, 50.1.